

EPR studies of some f n and d n electronic impurities in KTaO₃ single crystals

M. M. Abraham, L. A. Boatner, D. N. Olson, and U. T. Höchli

Citation: *The Journal of Chemical Physics* **81**, 2528 (1984); doi: 10.1063/1.447986

View online: <http://dx.doi.org/10.1063/1.447986>

View Table of Contents: <http://scitation.aip.org/content/aip/journal/jcp/81/6?ver=pdfcov>

Published by the [AIP Publishing](#)

Articles you may be interested in

[Electronspin resonance studies of the titanium cation \(Ti⁺, 3d³, 4 F\) in rare gas matrices at 4 K: A crystal field interpretation](#)

J. Chem. Phys. **105**, 5331 (1996); 10.1063/1.472401

[Epitaxial YBa₂Cu₃O₇ growth on KTaO₃ \(001\) single crystals](#)

Appl. Phys. Lett. **63**, 3376 (1993); 10.1063/1.110150

[An a b i n i t i o study of the collinear reaction of Fe⁺ \(4 F\) and Fe⁺ \(6 D\) with H₂](#)

J. Chem. Phys. **94**, 4352 (1991); 10.1063/1.460622

[Epitaxial superconducting thin films of YBa₂Cu₃O_{7-x} on KTaO₃ single crystals](#)

Appl. Phys. Lett. **54**, 1063 (1989); 10.1063/1.101426

[CALCIUM CONCENTRATION VS NET IONIZED DONOR CONCENTRATION IN SINGLECRYSTAL KTaO₃](#)

Appl. Phys. Lett. **8**, 173 (1966); 10.1063/1.1754540



AIP | Chaos

CALL FOR APPLICANTS

Seeking new Editor-in-Chief

EPR studies of some f^n and d^n electronic impurities in KTaO_3 single crystals^{a)}

M. M. Abraham and L. A. Boatner

Solid State Division, Oak Ridge National Laboratory, Oak Ridge, Tennessee 37830

D. N. Olson

St. Olaf College, Northfield, Minnesota 55057

U. T. Höchli

IBM Zurich Research Laboratory, CH-8803, Rüschlikon, Switzerland

(Received 8 March 1984; accepted 16 May 1984)

Single crystals of the cubic perovskite host, potassium tantalate (KTaO_3), doped with iron group, lanthanide, and actinide impurities have been investigated using the technique of electron paramagnetic resonance (EPR). The EPR spectra of Yb^{3+} and U^{5+} have been observed for the first time in potassium tantalate by employing crystals co-doped with both impurities. Multiple doping of the material during the crystal growth process avoided the production of semiconducting KTaO_3 and resulted in the incorporation of adequate concentrations of the trivalent lanthanide ion Yb^{3+} . The EPR results indicate that Yb^{3+} occupies a site in which the local symmetry is axial as a result of nearby charge compensation. Pentavalent uranium is found to occupy a substitutional cubic symmetry site. EPR investigations of Cu^{2+} , Co^{2+} , Mn^{2+} , Ni^{3+} , and Fe^{3+} were also carried out.

INTRODUCTION

Recent investigations of hydrogen diffusion in potassium tantalate (KTaO_3) and the interactive role played by transition-metal impurities^{1,2} have led to renewed interest in the solid state properties of doped tantalate crystals. In particular, work is currently in progress³ in which the effect of hydrogen on the high-temperature electrical properties of KTaO_3 is being investigated. In the specific case of Fe^{3+} in single crystals of KTaO_3 , it has been shown that the conditions resulting in the formation of OH^- in KTaO_3 also produce a significant change in the relative intensities of the cubic- and axial-site Fe^{3+} EPR spectra.² Accordingly, it is of interest to investigate the relationships between the properties of other transition-metal impurities and the diffusion of hydrogen. The purpose of the work reported here is to provide fundamental information regarding the local environments of f^n and d^n electronic impurities in KTaO_3 as a basis for future studies of the effects of hydrogen in doped tantalate crystals. In the present study, the EPR spectra of Yb^{3+} and U^{5+} in KTaO_3 were observed for the first time, and more complete EPR results are given for Cu^{2+} in KTaO_3 —a system that was the subject of an earlier preliminary report.⁴ Additionally, EPR spectroscopy was used in a reexamination of KTaO_3 doped with Co^{2+} , Mn^{2+} , and Ni^{3+} —ions that along with Eu^{2+} , Gd^{3+} , Fe^{3+} , and Ti^{3+} have been observed in earlier work.^{5–12}

EXPERIMENTAL

The single crystals of KTaO_3 employed in the present investigations were grown by means of a flux technique similar to that described by Hannon.^{5,13,14} High-purity tantalum oxide (Ta_2O_5) was combined with a slight stoichiometric excess of K_2CO_3 , and the compound KTaO_3 was formed by

reacting this mixture in a platinum crucible at $\approx 1420^\circ\text{C}$. Small amounts of the appropriate oxides were added to the mixture to furnish the desired impurities, and single crystals of KTaO_3 were grown by slowly cooling (1°C/h) the melt between the reaction temperature and 950°C . After cooling to room temperature, the self-nucleated crystals were removed from the remaining flux by dissolving the latter in hot H_2O .

A homodyne X-band spectrometer utilizing a Varian rectangular cavity with 100 kHz modulation was used for measurements between 77 K and room temperature. Two different EPR superheterodyne spectrometers operating at 3 cm (X band) and 1.2 cm (K band) were employed in the resonance studies at liquid helium temperatures. The applied magnetic field values were determined by means of a proton magnetic resonance probe, and both the proton resonance and the microwave frequencies were measured using a Hewlett Packard HP-5245L frequency counter with an HP-5255A frequency converter. Temperature stability was extremely important as the dielectric constant of the KTaO_3 samples changed drastically with minute changes in temperature, thereby affecting the cavity resonance frequency and the associated tuning of the spectrometer.

RESULTS AND DISCUSSIONS

General

The cubic perovskite KTaO_3 is a so-called incipient ferroelectric and does not undergo a ferroelectric (or structural) phase transition down to temperatures as low as 1.2 K. A cubic perovskite of the type ABO_3 may be visualized as a cube with six oxygen ions in the center of the faces, a B ion in the body center, and eight A ions at the corners. Thus, the A ion is dodecahedrally coordinated by oxygens (12 nearest-neighbor oxygen ions along the $\langle 110 \rangle$ axes) and the B ion is octahedrally coordinated by the oxygens (six nearest-neighbor oxygens along the $\langle 100 \rangle$ axes). Considerations of ionic

^{a)} Research sponsored by the Division of Materials Sciences, U. S. Department of Energy under contract W-7405-eng-26 with Union Carbide Corporation.

radii indicate that iron-group ions should substitute for the B ion and that rare-earth ions should reside in the A ion sites. In a review article, Müller¹⁵ has summarized the earlier data from electron paramagnetic resonance (EPR) studies of substitutional defects in ABO₃ type perovskites. He points out that in KTaO₃, Fe³⁺, and Ni³⁺ ions have been observed on K¹⁺ sites in addition to the "normal" Ta⁵⁺ site.⁵ Additionally, in the related fluoride perovskite, KMgF₃, Abraham *et al.*¹⁶ found that the rare-earth ions Yb³⁺, Tm²⁺, Er³⁺, and Dy³⁺ occupied the smaller Mg²⁺ ion site and not the larger K¹⁺ ion site. Accordingly, the possible occupation of either an A or B site by a given ion must be considered.

KTaO₃:Yb³⁺

For crystals of KTaO₃ doped only with ytterbium, no Yb³⁺ EPR signals were observed. When the crystals were co-doped with both ytterbium and uranium, however, an Yb³⁺ EPR spectrum was observed at 4.2 K. This spectrum exhibited tetragonal symmetry about the three (100) crystallographic axes. With the applied magnetic field parallel to a [100] axis, one of the three equivalent centers has $\theta = 0^\circ$. The other two centers both have $\theta = 90^\circ$ and, therefore, their EPR spectra coincide. The EPR spectrum with the applied H field perpendicular to the principal axis of the axial Yb³⁺ site is shown in Fig. 1. The intense line from the $I = 0$ isotopes and the lines exhibiting hyperfine structure from the ¹⁷¹Yb ($I = 1/2$, 14% natural abundance) and ¹⁷³Yb ($I = 5/2$, 16% natural abundance) isotopes are evident. The observed Yb³⁺ spectrum can be described by the usual axially symmetric spin Hamiltonian with $S = 1/2$, $g_{\parallel} = 4.775(2)$ and $g_{\perp} = 2.430(1)$, and the following hyperfine parameters: ¹⁷¹ $A_{\parallel}(1/2) = 3754(1)$ MHz [$1252.2(3) \times 10^{-4}$ cm⁻¹], ¹⁷¹ $A_{\perp}(1/2) = 1873(1)$ MHz [$624.8(3) \times 10^{-4}$ cm⁻¹], ¹⁷³ $A_{\parallel}(5/2) = 1035(1)$ MHz [$345.2(3) \times 10^{-4}$ cm⁻¹], and ¹⁷³ $A_{\perp}(5/2) = 517.8(5)$ MHz [$172.7(2) \times 10^{-4}$ cm⁻¹]. The ratio ¹⁷¹ $A_{\parallel}/^{173}A_{\parallel} = 3.627(3)$ is in good agreement with the ratio of the nuclear magnetic moments ¹⁷¹ $\mu/^{173}\mu = 3.630$. The Yb³⁺ EPR lines were not visible at a sample temperature of 77 K but could be observed at $T = 4.2$ K. As can be seen in Fig. 1, the lines saturated easily at 1.5 K. The linewidth with the applied magnetic field parallel to the axis of symmetry is 2.5 and 10 G when the field is perpendicular to this axis. No superhyperfine structure was visible.

Yb³⁺ has a $4f^{13}$ electronic configuration and a $^2F_{7/2}$ free-ion ground state. The eightfold ground-state degeneracy is split by a tetragonal crystal field into four Kramers' doublets, and the EPR spectrum observed at $T = 4.2$ K arises from transitions within the ground doublet.

The ionic radius of Yb³⁺ (0.94 Å), which is considerably larger than that of the Ta⁵⁺ ion (0.73 Å), suggests that the ytterbium would go into the 12-fold coordinated potassium site. If the crystal field were cubic at the two sites, then Yb³⁺ in the sixfold coordinated Ta⁵⁺ site would exhibit a ground Γ_6 doublet with an isotropic g value of approximately $8/3$. If the Yb³⁺ were in the 12-fold coordinated K¹⁺ site, the ground states would be either a Γ_7 doublet or a Γ_8 quartet. The former would be characterized by an isotropic g value of approximately $24/7$ while the latter would have anisotropic g values in the cubic field. Our experimental aver-

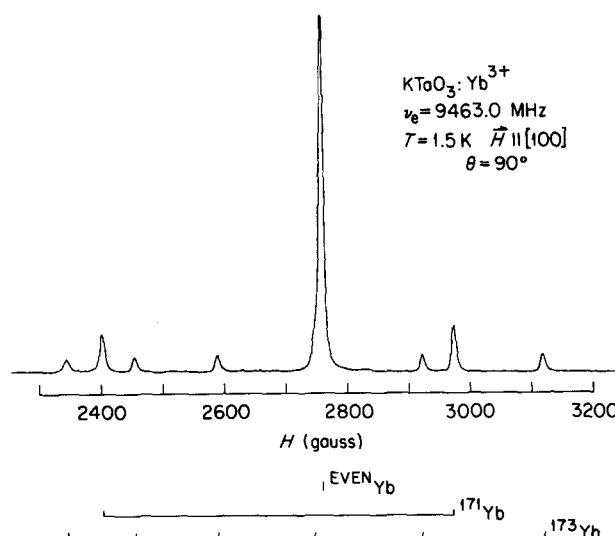


FIG. 1. EPR spectrum of KTaO₃:Yb³⁺ with $\theta = 90^\circ$. The hyperfine structure is depicted by the stick diagram beneath the experimental trace. No superhyperfine structure is observed.

age g value of 3.212 [$g_{av} = (g_{\parallel} + 2g_{\perp})/3$] can be considered to be the result of a small tetragonal distortion acting on a Γ_7 doublet in a cubic field. Therefore, the g values suggest that the ytterbium is in the K¹⁺ site. The Elliott and Stevens' parameter, ¹⁷ $g_{\parallel}A_{\perp}/g_{\perp}A_{\parallel}$, is 0.981 for ¹⁷¹Yb and 0.983 for ¹⁷³Yb. Since this is close to unity, it indicates that there are negligible admixtures from higher lying J states.

It is interesting to note that in KMgF₃ an isotropic Yb³⁺ spectrum was observed¹⁶ with $g = 2.584$. This spectrum is characteristic of Yb³⁺ in a Mg²⁺ sixfold-coordinated cubic site having a Γ_6 ground state. The ionic radius of Mg²⁺ (0.65 Å) is even lower than that of Ta⁵⁺ (0.73) and thus arguments based upon ionic size alone must be used with caution.

KTaO₃:U⁵⁺

The electronic configuration of U⁵⁺ is $5f^1$ with a free-ion ground state of $^2F_{5/2}$. A cubic crystal field will split the sixfold ground state degeneracy into a doublet and a quartet. In a Ta⁵⁺ site for which the nearest neighbor coordination is sixfold cubic, the predicted ground state is the Γ_7 doublet which is expected to have an isotropic g value of $g \approx 10/7$. In the 12-fold cubic coordinated K¹⁺ site, the ground state would be the Γ_8 quartet with g values that are anisotropic.

Experimentally, for uranium-doped KTaO₃ crystals, a line was observed at both 77 and 4.2 K with an isotropic g value of 0.616(2). The line had a FWHM of 75 G at 4.2 K when the magnetic field was parallel to a [100] axis and there was some indication of superhyperfine structure. Unfortunately, the resolution of this structure was lost when the field was rotated off of the [100] axis. The overall line width increased with increasing applied magnetic field angle so that the line could not be seen more than 20° away from a (100) axis. The line was attributed to U⁵⁺ in a Ta⁵⁺ site for the following reasons: First, no charge compensation is required for this site occupancy and the isotropic g value indicates

that the paramagnetic ion is in a cubic field. Second, the resonance could be seen at $T = 77$ K implying a relatively long relaxation time. Third, there is a close agreement in ionic size between U^{5+} and Ta^{5+} . Fourth, the reduction of the observed g value from the g value for a pure Γ_7 doublet can be explained on the basis of a crystal-field-induced admixture of a different Γ_7 state from the higher lying $J = 7/2$ manifold into the ground Γ_7 doublet. This is precisely the argument given by Reynolds *et al.*¹⁸ to account for the observed g values for the isoelectronic Ce^{3+} ion in the alkaline earth oxides.

Uranium-doped LiTaO_3 and LiNbO_3 (ilmenite structure) have been observed¹⁹ to exhibit broad room temperature spectra that were attributed to U^{5+} substituted for either Ta^{5+} or Nb^{5+} in octahedral sites. For U^{5+} in LiNbO_3 an isotropic line was observed with $g = 0.727$. This line had a 250 G linewidth which reduced to 120 G at $T = 7$ K. For U^{5+} in LiTaO_3 , an axial spectrum with $g_{\parallel} = 0.773$ and $g_{\perp} = 0.685$ was observed. Lewis *et al.*¹⁹ were unable to detect EPR in several uranium-doped perovskites including KTaO_3 . However, their samples were black and semiconducting. Here, uranium EPR spectra were only observed in crystals that were co-doped with ytterbium or dysprosium. The co-doped crystals were pale yellow in color and were not semiconducting.

KTaO₃:Cu²⁺

The EPR spectrum of Cu^{2+} in a KTaO_3 single crystal consisted of three axially symmetric spectra whose principal axes lay along the cubic fourfold axes of the KTaO_3 host crystal.⁴ As shown in Fig. 2, for $H \parallel [100]$ and at a sample temperature of 77 K, the spectrum consists of four major transitions which exhibit a strong resolved superhyperfine structure. In fact, eight transitions are present that originate from the two isotopes, ^{63}Cu and ^{65}Cu , both of which have a nuclear spin $I = 3/2$. The nuclear magnetic moments of these isotopes only differ by 10% and, therefore, the two four-line hyperfine patterns are not resolved in this case. The four transitions shown in Fig. 2 represent the spectrum asso-

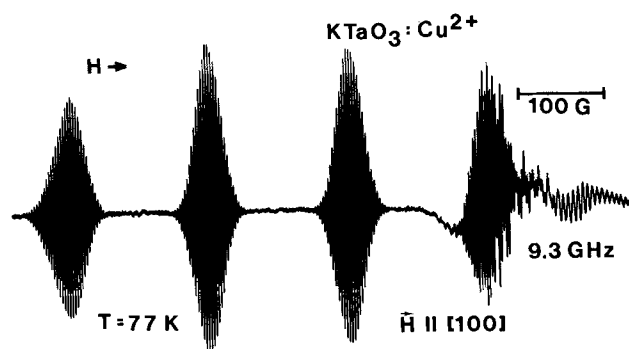


FIG. 2. EPR spectrum of a single crystal of $\text{KTaO}_3:\text{Cu}^{2+}$. The hyperfine structure for one of the three axially symmetric spectra with $\theta = 0^\circ$ is clearly resolved. The four lines are due to ^{63}Cu and ^{65}Cu (both $I = 3/2$) whose magnetic moments are not very different in magnitude. The hyperfine structure is not resolved for the doubly degenerate $\theta = 90^\circ$ spectra and this transition is superimposed upon the highest field hyperfine transition belonging to the $\theta = 0^\circ$ spectrum. Superhyperfine lines are clearly evident.

ciated with an orientation of the applied magnetic field parallel to the symmetry axis for one of the three tetragonally symmetric spectra. The Cu hyperfine structure is not resolved on the transitions for which the applied field is perpendicular to the principal axes of the two remaining spectra, and these superimposed spectra interfere with the superhyperfine structure of the fourth (counting from low field) Cu hyperfine transition of the spectrum corresponding to the parallel orientation. The observed tetragonally symmetric Cu^{2+} spectra are described by the usual axially symmetric spin Hamiltonian with $g_{\parallel} = 2.228(2)$, $g_{\perp} = 2.056(5)$, $^{63}A_{\parallel} = 173(2) \times 10^{-4} \text{ cm}^{-1}$ and $^{65}A_{\perp} = 45(3) \times 10^{-4} \text{ cm}^{-1}$.

Divalent copper has the $3d^9$ electronic configuration. For Cu^{2+} in a cubic sixfold coordinated site, an orbital electronic doublet is lowest and the Jahn–Teller effect should be observed. For a static Jahn–Teller effect, three tetragonally symmetric spectra identical to the observed spectra would be seen. If a static Jahn–Teller effect is operable, however, an averaging of the tetragonal spectra should occur with increasing temperature to produce an isotropic spectrum. No such averaging was in evidence and, in fact, the tetragonally symmetric spectra could still be observed (although with a decreased intensity) at room temperature. The tetragonal symmetry is, therefore, due to a defect (presumably an oxygen vacancy) associated with the Cu^{2+} ion. This would be consistent with Cu^{2+} occupying a Ta^{5+} site since the symmetry axes of the Cu^{2+} spectra are the $\langle 100 \rangle$ crystallographic directions. This model, however, does not provide for complete charge compensation. If the Cu^{2+} were to occupy a K^+ site with a K^+ vacancy in a next nearest-neighbor position (which would also produce the observed $\langle 100 \rangle$ axial symmetry) then, in this dodecahedrally coordinated K^+ site, the cubic crystal field would yield an orbital electronic triplet ground state. A tetragonal field splits this triplet and magnetic resonance transitions would occur between the spin levels of a resulting orbital singlet. In this case, however, the relaxation time would probably be too short for EPR spectra to be observed at room temperature. In addition, the experimental g values would be expected to be quite different from the free-electron value and both axial g values should not be greater than 2.0.

In an attempt to obtain a clearer picture of the superhyperfine structure evident in Fig. 2, a KTaO_3 crystal was grown with CuO which had been isotopically enriched to 99.7% ^{65}Cu . The EPR spectrum obtained using this sample is shown in Fig. 3. As expected, some simplification of the superhyperfine structure occurs when only one copper isotope is present in the doped crystal. The superhyperfine structure observed on the first and second of the four hyperfine transitions (counting from low field) is shown in Figs. 4 and 5 for KTaO_3 crystals doped with naturally abundant and isotopically enriched ^{65}Cu . A comparison of these figures shows that a reduced number of superhyperfine lines are present in the ^{65}Cu -doped sample. The origin of the superhyperfine structure, unfortunately is not definitively established. There appear to be more lines than would be expected for Cu^{2+} at a tantalum site with eight equivalent nearest-neighbor potassium ions $[2 \times (8 \times \frac{3}{2}) + 1 = 25]$ and fewer lines than would be expected at a potassium site with

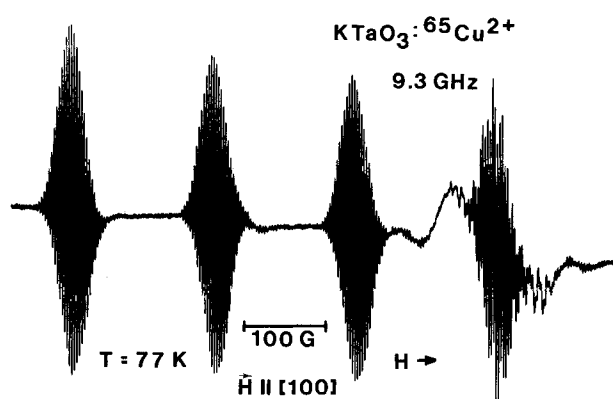


FIG. 3. EPR spectrum of KTaO_3 doped with 99.7% enriched ^{65}Cu . The Cu hyperfine structure is now due to only one isotope.

eight equivalent nearest-neighbor tantalum ions [$2 \times (8 \times \frac{3}{2}) + 1 = 57$]. (Potassium has two isotopes, 93% abundant ^{39}K and 7% abundant ^{41}K , with magnetic moments $^{39}\mu = 0.3914$ and $^{41}\mu = 0.2149$. This can lead to further complications but the larger moment for the more abundant isotope and the regularity of the observed pattern probably makes this inclusion unnecessary.) The excess number of lines does not present a serious problem for a tantalum site assignment, since contributions from next nearest-neighbor (tantalum) ions can be comparable to the nearest-neighbor (potassium) ions. Copper doped single crystals of KTaO_3 were prepared in which various amounts of either Na (substituting for potassium) or Nb (substituting for Ta) were incorporated in the samples. EPR spectra of these mixed crystals were obtained in an attempt to establish whether the origin of the observed superhyperfine structure

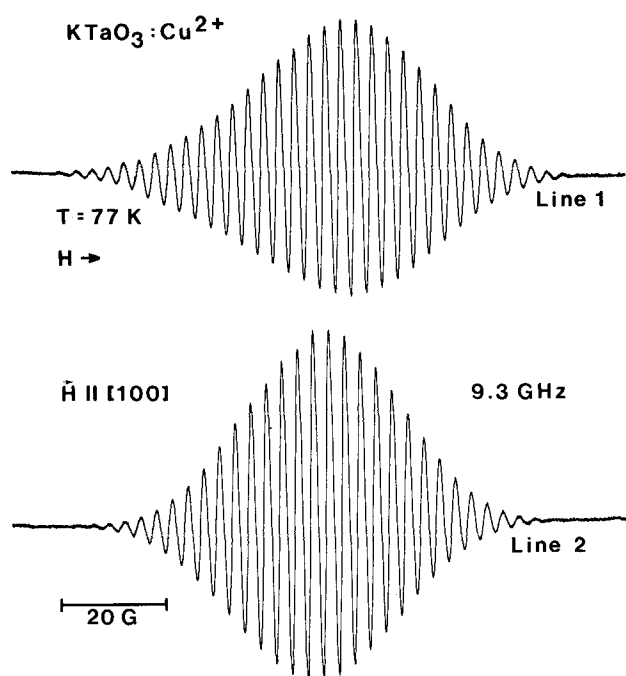


FIG. 4. Superhyperfine lines in $\text{KTaO}_3:\text{Cu}$. The two lowest field hyperfine transitions for $\theta = 0^\circ$ in naturally abundant Cu-doped KTaO_3 [see Fig. 2] are shown with high resolution.

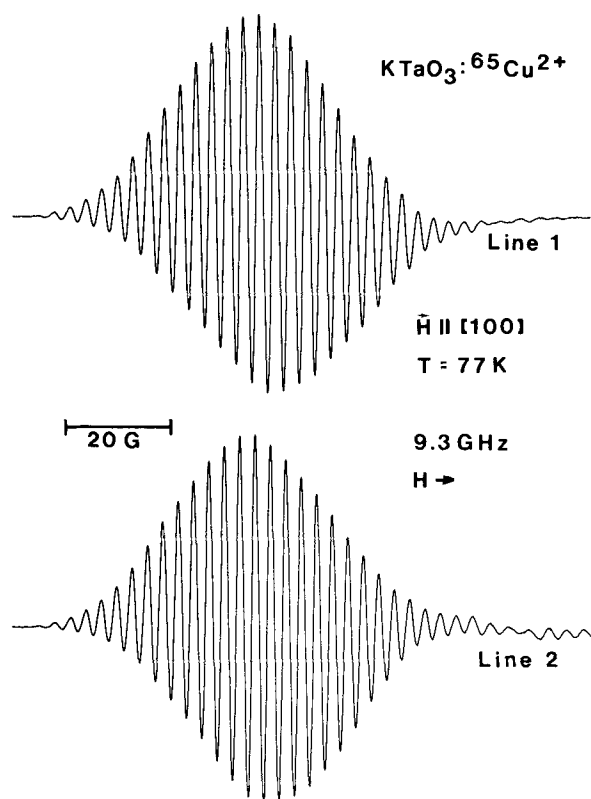


FIG. 5. Superhyperfine lines in $\text{KTaO}_3:^{65}\text{Cu}$. The two lowest field hyperfine transitions for $\theta = 0^\circ$ in KTaO_3 doped with 99.7% enriched ^{65}Cu are shown with high resolution.

was potassium or tantalum. Alterations of the superhyperfine structure were observed when either Na or Nb was incorporated in the Cu-doped crystals, however.

We have attempted to perform ENDOR experiments on the superhyperfine structure at 4.2 K. These experiments were unsuccessful since the EPR lines had relatively short relaxation times and could not be saturated with the available microwave power.

$\text{KTaO}_3:\text{Co}^{2+}$

The spectrum shown in Fig. 6 was observed at 4.2 K for crystals of $\text{KTaO}_3:\text{Co}^{2+}$. The eight-line hyperfine structure due to the 100% abundant ^{59}Co nucleus is clearly evident, and the spectrum exhibited axial symmetry about the three $\langle 100 \rangle$ axes of the crystal. The positions of the lines were described by the spin Hamiltonian

$$\mathcal{H} = g_{\parallel} \mu_B H_z S_z + g_{\perp} \mu_B (H_x S_x + H_y S_y) + A_{\parallel} S_z I_z + A_{\perp} (S_x I_x + S_y I_y), \quad (1)$$

with $S = 1/2$, $I = 7/2$, $g_{\parallel} = 2.067(1)$, $g_{\perp} = 4.958(2)$, $^{59}A_{\parallel} = 174.5(5)$ MHz [$58.2(2) \times 10^{-4} \text{ cm}^{-1}$], and $^{59}A_{\perp} = 221(1)$ MHz [$73.7(3) \times 10^{-4} \text{ cm}^{-1}$]. These values are in reasonable agreement with those obtained by Hannon¹¹ who identified the spectrum as arising from a Co^{2+} ion residing in a Ta^{5+} site with a nearest-neighbor oxygen vacancy. (Of course, further charge compensation is necessary in order to preserve electrical neutrality.) The two possible impurity sites in the KTaO_3 perovskite lattice, the K^{1+} and Ta^{5+} sites, have opposite signs for the fourth order cubic-field splitting pa-

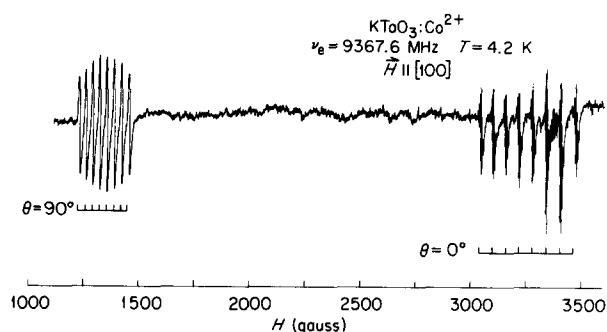


FIG. 6. EPR spectrum of a single crystal of $\text{KTaO}_3:\text{Co}^{2+}$. The spectrum is shown for $H \parallel [100]$. The high field group of eight lines for the $I = 7/2$ nuclear spin of the ^{59}Co nucleus is due to sites oriented parallel to the field, while the low field group of lines is due to sites oriented perpendicular to the field and is doubly degenerate. Superhyperfine structure can be seen on the $\theta = 0^\circ$ lines.

rameter. The ground state of the Co^{2+} ion with a d^7 electronic configuration has a sevenfold orbital degeneracy which is split by a cubic crystal field into a singlet and two triplets. For 12-fold cubic coordination the orbital singlet would be lowest, whereas for sixfold cubic coordination the orbital triplet would be lowest. The experimental fact that the Co^{2+} EPR spectrum is not observed at liquid nitrogen temperature argues for a short spin lattice relaxation time associated with an orbital triplet ground state and, hence, we conclude that the Ta^{5+} site is also the correct one for Co^{2+} .

The observed superhyperfine interaction, due to the surrounding nuclei, exhibits the best resolution when the external magnetic field is applied along a $[100]$ symmetry axis (as can be seen in Fig. 6). The odd number of superhyperfine lines indicates that interactions occur with an even number of equivalent nuclei in this direction, but a definitive identification of the origin of the superhyperfine structure was not made.

$\text{KTaO}_3:\text{Mn}^{2+}$

In the case of KTaO_3 doped with manganese, the spectrum shown in Fig. 7 was observed when the applied magnetic field was aligned along one of the $\langle 100 \rangle$ axes. The spectrum consists of three sets of five groups of lines, with each group divided into six lines by a hyperfine interaction. The three sets exhibit axial symmetry and with H parallel to a $[100]$ crystallographic direction, the magnetic field is parallel to a symmetry axis for one site and perpendicular to the symmetry axes for the remaining two sites. (At $\theta = 0^\circ$, the highest group of hyperfine lines lies above the high magnetic field limit of the spectrometer and, hence, does not appear in the figure.) The spectra can be described by the following spin Hamiltonian:

$$\begin{aligned} \mathcal{H} = & g_{\parallel} \mu_B H_z S_z + g_{\perp} \mu_B (H_x S_x + H_y S_y) \\ & + (b_2^0/3) 0_2^0 + (b_4^0/60) 0_4^0 \\ & + (b_4^4/60) 0_4^4 + A_{\parallel} I_z S_z + A_{\perp} (I_x S_x + I_y S_y) \quad (2) \end{aligned}$$

with $S = 5/2$, $I = 5/2$, $g_{\parallel} = 1.9978(5)$, $g_{\perp} = 2.0004(5)$, $b_2^0 = 1480(1) \times 10^{-4} \text{ cm}^{-1}$, $b_4^0 = -1.2(4) \times 10^{-4} \text{ cm}^{-1}$, b_4^4

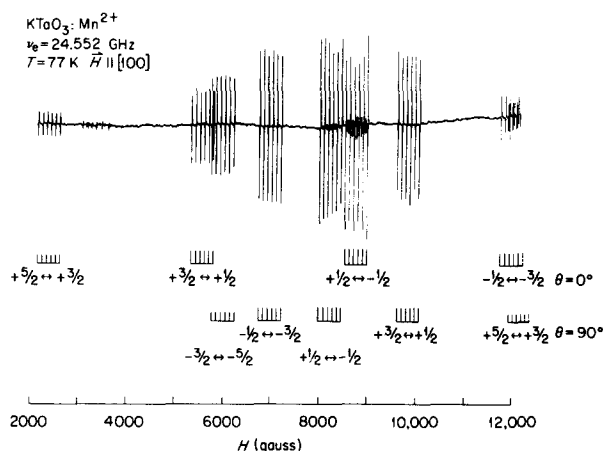


FIG. 7. EPR spectrum of a single crystal of $\text{KTaO}_3:\text{Mn}^{2+}$. The spectrum is shown for an orientation of the applied magnetic field parallel to a $[100]$ direction. One of the three magnetically equivalent sites is oriented parallel to the field, $\theta = 0^\circ$ while the other two sites are oriented perpendicular to the field, $\theta = 90^\circ$. The resonance transitions are labeled by the stick diagram beneath the experimental trace. The fine structure group $M_s = -3/2 \leftrightarrow M_s = -5/2$ at high field for $\theta = 0^\circ$ is not shown due to the limitations of the laboratory magnetic field.

$= +2(2) \times 10^{-4} \text{ cm}^{-1}$, $^{55}A_{\parallel} = 85.9(4) \times 10^{-4} \text{ cm}^{-1}$, $^{55}A_{\perp} = 82.7(4) \times 10^{-4} \text{ cm}^{-1}$. The above parameters were determined for a sample temperature of 77 K, and the absolute signs were determined by comparing the intensities of the lines at 4.2 K. No other manganese spectrum was detected. Except for minor differences, the center reported here seems to agree with the results of Hannon⁵ who concluded that the Mn^{2+} was in a Ta^{5+} site with an adjacent O^{2-} vacancy. His arguments were based on the following four points: (1) the relative ionic sizes, (2) the known tendency of KTaO_3 to grow with oxygen deficiencies and the observed $[100]$ direction of the axial distortion, (3) the large value of b_2^0 , and (4) the effect of co-doping with titanium. Crystals co-doped with titanium and manganese showed no divalent manganese EPR spectrum. Hannon explained this observation by arguing that Ti^{4+} entered the Ta^{5+} site preferentially and forced the Mn^{2+} either to go elsewhere in the lattice or to change its valence. Geifman²⁰ noted that the potassium content in KTaO_3 was higher in crystals containing manganese relative to undoped "pure" samples. This is additional evidence for divalent manganese occupying the Ta^{5+} site.

$\text{KTaO}_3:\text{Fe}^{3+}$ and Ni^{3+}

Spectra were observed for several crystals of KTaO_3 doped with nickel. Different sites with axial symmetry aligned along the crystallographic $\langle 100 \rangle$ axes were observed with the experimental g values listed in Table I. The sites labeled I and II, seen in lightly doped crystals at 77 K, appear to be the centers reported by Hannon⁵ and attributed to Ni^{3+} substituted, respectively, for K^+ and Ta^{5+} ions with adjacent O^{2-} vacancies. The lines for site II appeared to saturate more readily than those for site I. Neither center showed evidence of superhyperfine structure. The ground state of Ni^{3+} ion has a d^7 electronic configuration and therefore has an F orbital ground state. This sevenfold orbital

TABLE I. Spin Hamiltonian parameters.

Ion	g	g	Fine structure ($\times 10^{-4} \text{ cm}^{-1}$)	Hyperfine constant (10^{-4} cm^{-1})	Temp.
Yb ³⁺	4.775(2)	2.430(1)		¹⁷¹ A (1/2) = 1252.2(3), ¹⁷¹ A (1/2) = 624.8(3) ¹⁷³ A (5/2) = 345.2(3), ¹⁷³ A (5/2) = 172.7(2)	4.2 K 4.2 K
U ⁵⁺	$g_{\text{iso}} = 0.616(2)$				77 K
Cu ²⁺	2.228(2)	2.056(5)		⁶⁵ A (3/2) = 173(2), ⁶⁵ A (3/2) = 45(3)	77 K
Co ²⁺	2.067(1)	4.958(2)		⁵⁹ A (7/2) = 58.2(2), ⁵⁹ A (7/2) = 73.7(3)	4.2 K
Mn ²⁺	1.9978(5)	2.0004(5)	$b_2^0 = +1480(1)$ $b_4^0 = -1.2(4)$ $b_4^4 = +2(2)$	⁵⁵ A (5/2) = 85.9(4), ⁵⁵ A (5/2) = 82.7(4)	77 K
Ni ³⁺ I	2.219(1)	4.430(2)			77 K
Ni ³⁺ II	2.236(2)	2.116(2)			77 K
Fe ³⁺	1.997(1)	6.007(6)			77 K
Fe ³⁺ or Ni ³⁺ III	1.968(2)	4.337(2)			77 K

degeneracy is split into a singlet and two triplets by a cubic crystal field. In a K⁺ site, the singlet would be lowest while in a Ta⁵⁺ site a triplet would be lowest. On the basis of the g values, it appears to us that center II originates from nickel in the K⁺ site and center I from nickel in the Ta⁵⁺ site which is contrary to Hannon's conclusions.⁵

Surprisingly, the spectra for these sites (I and II) were difficult to detect in a heavily doped nickel sample. The heavily doped sample exhibited an additional (100) axial center labeled III at both $T = 77 \text{ K}$ and $T = 4.2 \text{ K}$. A strong superhyperfine structure was observed which was best resolved when the magnetic field was applied either parallel or perpendicular to the symmetry axis. Unfortunately, the resolution was inadequate for detailed analysis. An axial Fe³⁺ center was observed in the heavily doped Ni samples with $g_{\parallel} = 1.997(1)$ and $g_{\perp} = 6.007(6)$ which corresponds to the Fe³⁺ spectrum observed by Wessel and Goldick⁹ and Hannon⁵ and which was attributed to an Fe³⁺ in a Ta⁵⁺ site with a nearby oxygen vacancy. Using variable frequencies between 30 and 75 GHz, Wessel and Goldick⁹ determined the zero field splitting of this axial Fe³⁺ center to be 2.88 cm^{-1} . They also observed a second axial Fe³⁺ center with a smaller zero field splitting of 0.74 cm^{-1} . It is possible that the values obtained here for the center labeled III at X-band frequencies may be due to this second iron center. The spectra of center III and the known axial iron center both exhibited superhyperfine structure while the spectra attributed to nickel (I and II) did not.

SUMMARY

Previous investigations of KTaO₃ single crystals doped with iron have shown that, depending on the redox conditions experienced by the material, trivalent iron will occupy either a cubic substitutional site or an axial site that results from a distortion of the cubic symmetry by nearby charge compensation. This earlier work also established that significant changes in the relative intensities of the cubic and axial site EPR spectra of Fe³⁺ in KTaO₃ were produced by the same conditions that resulted in either the incorporation in or removal of OH⁻ from the material. These results have led to renewed interest in the role played by hydrogen in determining the solid state chemical and high temperature electri-

cal properties of KTaO₃. In particular, the solid state chemical properties of impurities other than iron group ions and the effects of hydrogen diffusion on the charge compensation mechanisms in KTaO₃ are of interest. In the present work, the two systems KTaO₃:Yb and KTaO₃:U have been investigated using EPR techniques. The results show that these systems represent, first, a case where the inherently trivalent ytterbium ion only occupies an axially symmetric site with local charge compensation in the "as-grown" crystals and, second, a case where the ion U⁵⁺, an ion that is isoivalent with Ta in KTaO₃, is located in a site of cubic symmetry. Accordingly, KTaO₃:Yb³⁺ and KTaO₃:U⁵⁺ represent two new systems whose properties differ from those of KTaO₃:Fe³⁺.

When doped with impurities, KTaO₃ appears to have a tolerance for misfits in ionic size and charge not normally found in other crystals. We attribute this property to the relatively large polarizability of the oxygen ionic shell which allows for considerable distortion and which has been shown to be responsible for incipient ferroelectricity in this crystal.²¹ Accordingly, the coherence length²² of the polarization is unusually large, and the associated screening effects reduce the Coulombic energy due to incomplete charge compensation.

The fundamental spectroscopic information provided by the present investigations of these systems will be used as a basis for extended studies of the solid state chemical effects associated with the incorporation of hydrogen in KTaO₃. Additional spectroscopic data are also reported for Cu²⁺, Co²⁺, Mn²⁺, Ni³⁺, and Fe³⁺ in KTaO₃ single crystals.

¹H. Engstrom, J. B. Bates, and L. A. Boatner, J. Chem. Phys. 73, 1073 (1980).

²R. Gonzalez, M. M. Abraham, L. A. Boatner, and Y. Chen, J. Chem. Phys. 78, 660 (1983).

³A. S. Nowick and W.-K. Lee (private communication).

⁴L. A. Boatner, A.-H. Kayal, and U. T. Höchli, Helv. Phys. Acta 50, 167 (1977).

⁵D. M. Hannon, Phys. Rev. 164, 366 (1967).

⁶I. N. Geifman, Phys. Status Solidi B 85, K5 (1978).

- ⁷D. M. Hannon, Phys. Rev. B **3**, 2153 (1971).
⁸S. H. Wemple, Ph.D. thesis, Massachusetts Institute of Technology, Cambridge, Massachusetts, 1963 (unpublished).
⁹G. Wessel and H. Goldick, J. Appl. Phys. **39**, 4855 (1968).
¹⁰D. Rytz, U. T. Höchli, K. A. Müller, W. Berlinger, and L. A. Boatner, J. Phys. C **15**, 3371 (1982).
¹¹D. M. Hannon, Phys. Status Solidi B **43**, K21 (1971).
¹²H. Unoki and T. Sakudo, J. Phys. Soc. Jpn. **21**, 1730 (1966).
¹³S. H. Wemple, Phys. Rev. A **137**, 1575 (1965).
¹⁴D. M. Hannon, Air Force Cambridge Research Laboratory (Bedford, Massachusetts) Scientific Report No. 7, AFCRL-66-303, (1966).
¹⁵K. A. Müller, J. Phys. (Paris) **42**, 551 (1981).
¹⁶M. M. Abraham, C. B. Finch, J. L. Kolopus, and J. T. Lewis, Phys. Rev. **3**, 2855 (1971).
¹⁷R. J. Elliott and K. W. H. Stevens, Proc. R. Soc. London Ser. A **218**, 553 (1953).
¹⁸R. W. Reynolds, Y. Chen, L. A. Boatner, and M. M. Abraham, Phys. Rev. Lett. **29**, 18 (1972).
¹⁹W. B. Lewis, H. G. Hecht, and M. P. Eastman, Inorg. Chem. **12**, 1634 (1973).
²⁰I. N. Geifman, Fiz. Tverd. Tela **23**, 1253 (1981) [Sov. Phys. Solid State **23**, 738 (1981)].
²¹R. Migoni, H. Bilz, and D. Bäuerle, Phys. Rev. Lett. **11**, 1155 (1976).
²²M. E. Lines, Phys. Rev. B **5**, 3690 (1972).